Plane-wave and common-translation-factor treatments of $He^{2+}+H$ collisions at high velocities

L. F. Errea
Departamento de Química, C-XIV, Universidad Autónoma de Madrid, Canto Blanco, 28049 Madrid, Spain

C. Harel and H. Jouin
Laboratoire des Collisions Atomiques, Université Bordeaux I, 351 Cours de la Libération, 33405 Talence, France

J. M. Maidagan and L. Méndez
Departamento de Química, C-XIV, Universidad Autónoma de Madrid, Canto Blanco, 28049 Madrid, Spain

B. Pons
Laboratoire des Collisions Atomiques, Université Bordeaux I, 351 Cours de la Libération, 33405 Talence, France

A. Riera
Departamento de Química, C-XIV, Universidad Autónoma de Madrid, Canto Blanco, 28049 Madrid, Spain
(Received 7 May 1992)

We complement previous work that showed that the molecular approach, modified with plane-wave translation factors, is able to reproduce the fall of charge-exchange cross sections in $He^{2+}+H$ collisions, by presenting the molecular data, and studying the corresponding mechanism. We test the accuracy of simplifications of the method that have been employed in the literature, and that lead to very simple calculations. We show that the common-translation-factor method is also successful at high nuclear velocities, provided that sufficiently excited states are included in the basis; moreover, it yields a simple picture of the mechanism and a description of ionization processes at high velocities.

PACS number(s): 34.70.+e, 34.50.Fa, 34.10.+x

I. INTRODUCTION

The molecular method, modified with the inclusion of translation factors [1,2], is a standard approach in the treatment of atomic collisions up to the energy region where charge-exchange cross sections are maximal. For higher energies, this method has usually been found (as stressed, e.g., in Refs. [3] and [4]) to fail to reproduce the drop of these cross sections with E. It is then worth investigating whether this failure is an intrinsic defect of the molecular method, either employing common [2] (CTF) or state-dependent, such as plane-wave [1] (PWTF), translation factors.

In a recent letter [5] we reported an extension to nuclear velocities as high as 2.8 a.u. of the PWTF work of Hatton, Lane, and Winter [6] and Winter and Hatton [7] on the benchmark $He^{2+}+H$ and $He^{+}+H^{+}$ collisions. Our main conclusion was that the correct overall behavior of total and partial charge-exchange cross sections beyond their maximum is obtained, well into the energy region where ionization dominates. The aims of the present work are (1) to complete the brief account given in Ref. [5], by presenting the relevant molecular and collisional data for $He^{2+}+H$ in detail; (2) to show that the CTF approach is also successful at high energies, by reporting calculations using factors that are specifically built for this energy region; (3) to elucidate the mechanisms that are responsible for the fall of the cross sections in both approaches; and (4) to conclude on the usefulness of these approaches as well as of that of other simplified procedures, which are very easy to implement.

Before presenting the theory, it is worth mentioning some aspects of the methods we shall employ.

CTF method. In order to describe $He^{2+}+H$ collisions for $v>1$ a.u., it has been shown [8] that the CTF approach requires augmenting the molecular-orbital (MO) basis further than those functions representing the entrance and the most relevant exit channels (what may be called a minimal MO basis). This was done in Ref. [8] through the introduction of pseudostates, called "probability absorbers," that account for probability flux towards states not included in the minimal MO basis. At large internuclear distances most of those absorbers were found to be superpositions of excited and continuum states, with energies close to the ionization threshold. It seems worth studying how well they can be approximated by additional excited states, and working out the ensuing mechanism of probability flow. For this purpose, we have performed calculations involving very large, as well as small, bases. Notice that the pessimistic conclusions of Refs. [3] and [4] for $v>1$ a.u. were drawn from minimal-basis calculations that did not include such excited states, and that employed CTF's determined for small velocities.

PWTF method. It was found in Ref. [9] that PWTF calculations are exceedingly time consuming. This conclusion was due to a somewhat purist approach in that it was exactly taken into account that our molecular wave functions were approximate—since in order to employ

the integration techniques proposed in Ref. [10], we used expansions in terms of Gaussian orbitals of the exact MO's. In practice, the cross-section calculations can be considerably speeded up, by assuming that one deals with exact eigenfunctions. We have checked that this approximation was sufficiently accurate for the five-state basis calculation reported in Ref. [5], but not for higher excited MO's. Therefore our present PWTF study is limited to such a minimal basis.

Even within the approximation of exact MO's and because of the nonfactorizable impact-parameter dependence of coupling matrix elements PWTF calculations are still considerably slower than CTF ones and this is one of the reasons why the latter approach has been much more employed than the former. This fact motivated us to investigate the accuracy of two methods that are sometimes employed, and that may be considered as (rather drastic) approximations to the PWTF approach that lead to calculations that are even simpler than CTF ones.

PS method. This procedure, suggested by Piacentini and Salin [11], ascribes to all molecular states the PWTF that corresponds to the entrance channel, by assuming that the electron "retains" its initial momentum throughout the collision. In practice, this is equivalent to employing a molecular approach without translation factors, and choosing the origin of electronic coordinates at the nucleus where the electron is initially bound.

$v^{(1)}$ method. Another possibility is, as first suggested by Bates and McCarroll [1] (see also Ref. [12]), to set $v=0$ in all momentum transfer phases $\exp\langle \pm i\mathbf{v}\cdot\mathbf{r}\rangle$ that appear in the integrands of the matrix elements of the PWTF treatment (see the following section). This is equivalent in practice to disregarding the translation factors in the molecular approach, and choosing different origins of electronic coordinates for different couplings, such that they all vanish at infinite internuclear separation. Since no other couplings than those linear in v remain, the method is sometimes referred to as the linear $v^{(1)}$ approximation to the PWTF approach.

As is well known, the latter two methods suffer from drawbacks. For example, in the PS method state-to-state electron-transfer probabilities oscillate, in general, as the atoms separate, and can therefore only be given with error bars; also, partial cross sections do not fulfill detailed balancing. Similarly, the $v^{(1)}$ method suffers from loss of unitarity, and therefore does not fulfill [13] detailed balancing either. Our interest here will not lie on these points, or on how cogent the methods are, but on the practical aspect of how accurate the total charge-exchange cross sections obtained are, which is a question that, to our knowledge, has not been investigated.

In the following section we introduce the basic equations of the different methods that are useful for the following discussion. We show in Sec. III the molecular data employed in the collisional treatments. Results of dynamical calculations are given in Sec. IV. The characteristics of the PWTF and CTF approaches at high velocities are discussed in Sec. V, and our main conclusions summarized in Sec. VI. Atomic units are used unless otherwise stated.

II. THEORY

A. PWTF method

As in our previous work [5], we use an impact-parameter formalism, and expand the electronic wave function in terms of a finite set of traveling MO's (TMO's) Φ_n of the HeH^{2+} system:

$$\Psi=\sum_n a_n\Phi_n \tag{1}$$

where

$$\Phi_n^A=\chi_n^A e^{-(i/2)\mathbf{v}\cdot\mathbf{r}}-i\int_0^t dt'(E_n+v^2/8)\ , \tag{2}$$

$$\Phi_m^B=\chi_M^B e^{(i/2)\mathbf{v}\cdot\mathbf{r}}-i\int_0^t dt'(E_m+v^2/8) \tag{3}$$

with $\mathbf{r}$ the electronic coordinate with respect to an origin placed midway between the nuclei, $\mathbf{v}$ the nuclear relative velocity, and $\chi_n^{A,B}$ the eigenfunctions of the electronic Hamiltonian H_{el}:

$$H_{el}\chi_n=E_n\chi_n\ . \tag{4}$$

In the following, whenever necessary these MO's χ_n will be ascribed a superscript A or B, depending upon whether they tend, at infinite internuclear separation R, to an atomic orbital of A (He^+ ion) or B (H atom):

$$\begin{aligned}&\lim_{R\to\infty}\chi_n^A=\phi_n^A\ ,\\ &\lim_{R\to\infty}\chi_m^B=\phi_m^B\ .\end{aligned} \tag{5}$$

Introduction of (1) in the impact-parameter equation leads, in a standard way, to a system of coupled differential equations for the expansion coefficients:

$$ie^{i\omega}\mathbf{S}e^{-i\omega}\dot{\mathbf{a}}=e^{i\omega}\mathbf{G}e^{-i\omega}\mathbf{a}\ , \tag{6}$$

where $\omega_{nm}=\delta_{nm}\int_0^t E_n(t')dt'$ and these matrices can be written in a partitioned form:

$$\mathbf{S}=\left[\begin{array}{c|c}\mathbf{S}^{AA} & \mathbf{S}^{AB}\\ \hline \mathbf{S}^{BA} & \mathbf{S}^{BB}\end{array}\right]\ ,\quad \mathbf{G}=\left[\begin{array}{c|c}\mathbf{G}^{AA} & \mathbf{G}^{AB}\\ \hline \mathbf{G}^{BA} & \mathbf{G}^{BB}\end{array}\right] \tag{7}$$

with

$$S_{nm}^{AA}=S_{nm}^{BB}=\delta_{n,m}\ , \tag{8}$$

$$S_{nm}^{AB}=S_{mn}^{BA\,*}=\int e^{i\mathbf{v}\cdot\mathbf{r}}\chi_n^A\chi_m^B\,d\mathbf{r}\ , \tag{9}$$

$$G_{nm}^{AA}=-i\int\chi_n^A\frac{\partial}{\partial t}\bigg|_{\mathbf{r}_A}\chi_m^A\,d\mathbf{r}\ , \tag{10}$$

$$G_{nm}^{BB}=-i\int\chi_n^B\frac{\partial}{\partial t}\bigg|_{\mathbf{r}_B}\chi_m^B\,d\mathbf{r}\ , \tag{11}$$

$$G_{nm}^{AB}=-i\int e^{i\mathbf{v}\cdot\mathbf{r}}\chi_n^A\frac{\partial}{\partial t}\bigg|_{\mathbf{r}_B}\chi_m^B\,d\mathbf{r}\ , \tag{12}$$

$$G_{nm}^{BA}=-i\int e^{-i\mathbf{v}\cdot\mathbf{r}}\chi_n^B\frac{\partial}{\partial t}\bigg|_{\mathbf{r}_A}\chi_m^A\,d\mathbf{r}\ . \tag{13}$$

Matrix elements of the type of (8), (10), and (11) are usually called of the direct kind, and also appear in the origi-

nal molecular treatment without translation factors. This is not so for matrix elements of type (9), (12), and (13), which involve in the integrand a phase $\exp(\pm i\mathbf{v}\cdot\mathbf{r})$. This phase may be considered as representing a local transfer of momentum: When the electron passes from being represented by the oribital χ^A to being described by χ^B, at the same point of space, its translation factor is shifted from being $\exp[-(i/2)\mathbf{v}\cdot\mathbf{r}]$ (momentum $-v/2$) to $\exp[(i/2)\mathbf{v}\cdot\mathbf{r}]$ (momentum $+v/2$), and this gives rise to the $\exp(i\mathbf{v}\cdot\mathbf{r})$ phase. The strong oscillation of this phase, at large energies, results in a vanishing of momentum transfer matrix elements. In particular, as $v\to\infty$ the overlap matrix $\mathbf{S}\to\mathbf{I}$ and $\mathbf{G}$ becomes block diagonal.

To solve Eq. (6), we first write it in the form

$$i\dot{\mathbf{a}}=e^{i\omega}\mathbf{S}^{-1}\mathbf{G}e^{-i\omega}\mathbf{a}\ , \tag{14}$$

and then the usual integration programs [14] can be employed, except that a (time-consuming) b- and v-dependent interpolation of the coupling matrix $\mathbf{S}^{-1}\mathbf{G}$ must be performed [9].

B. CTF method

In this approach, the total electronic wave function is expanded in the molecular basis set as follows [2]:

$$\Psi=e^{iU}\sum_n a_n\chi_n\exp\left[-i\int_0^t E_n dt'\right]\ , \tag{15}$$

where in the CTF phase the usual form for $U(\mathbf{r},t)$, involving a switching factor $f(\mathbf{r},R)$, was chosen

$$U(\mathbf{r},t)=f(\mathbf{r},R)\mathbf{v}\cdot\mathbf{r}-\tfrac{1}{2}f^2(\mathbf{r},R)v^2t\ . \tag{16}$$

The CTF introduces an effective electronic momentum which is the same for all states but differs from one point of space to another. The mechanism of charge transfer does not involve local transfer of momentum, but a variation of the electron flux (velocity times total electronic density) because of the modification of the MO's, which cause changes in energies and couplings.

Introduction of expansion (15) in the impact-parameter equation leads to the set of coupled equations:

$$i\dot{\mathbf{a}}=e^{i\omega}\mathbf{M}e^{-i\omega}\mathbf{a} \tag{17}$$

with

$$\begin{aligned}M_{mn}&=\left\langle e^{iu}\chi_m\left|H_{\rm el}-i\frac{\partial}{\partial t}\right|_{\rm r}\right|e^{iu}\chi_n\right\rangle-E_n\delta_{nm}\\&=\frac{v^2}{R^2}[(\mathbf{R}\cdot\hat{\mathbf{v}})^2+b^2U_{mn}-b(\mathbf{R}\cdot\hat{\mathbf{v}})W_{mn}]\\&\quad-i\frac{v}{R}(\mathbf{R}\cdot\hat{\mathbf{v}})\left[\left\langle\chi_m\left|\frac{\partial}{\partial R}\right|_{\rm r}\right|\chi_n\right\rangle-Z_{mn}\right]\\&\quad-i\frac{bv}{R^2}[\langle\chi_m|i\langle y|_0|\chi_n\rangle-X_{mn}]\ ,\end{aligned} \tag{18}$$

where ω is as in Eq. (6), b is the impact parameter, and the matrices $\mathbf{U}$, $\mathbf{V}$, $\mathbf{W}$, $\mathbf{X}$, and $\mathbf{Z}$ only depend upon the internuclear distance R; their explicit form in terms of the switching function $f(\mathbf{r},R)$ is not given here for the sake of conciseness. The main corrections to the radial and rotational dynamical couplings introduced by the CTF are proportional to the relative nuclear velocity v, and appear in the imaginary part of the coupling matrix $\mathbf{M}$. The real part of the diagonal of this matrix contains the corrections to the energies, which are $O(v^2)$.

As in Refs. [15, 16] the molecular wave functions employed in the CTF calculations are exact eigenfunctions of the molecular electronic Hamiltonian (OEDM orbitals) which are expressed in terms of prolate spheroidal coordinates $\{\lambda,\mu,\phi\}$, and the switching function f of Eq. (16) has the form [15]

$$f(\mathbf{r},R)=\tfrac{1}{2}\mu\alpha^{\alpha/2}(\alpha-1+\mu^2)^{-\alpha/2} \tag{19}$$

with $\alpha>1$ an adjustable parameter, which is related to the gradient $S=\partial f/\partial\mu$ at $\mu=0$ through $S=\frac{1}{2}[\alpha/(\alpha-1)]^{\alpha/2}$.

With respect to our previous, simpler choices [9] the factor (18) has the characteristics of not involving a cutoff factor at small R, and presenting a stationary value at each nuclear position ($\mu=\pm1$); we have shown [17] that a CTF must fulfill this latter condition when partial cross sections are to be evaluated. Changing the value of the

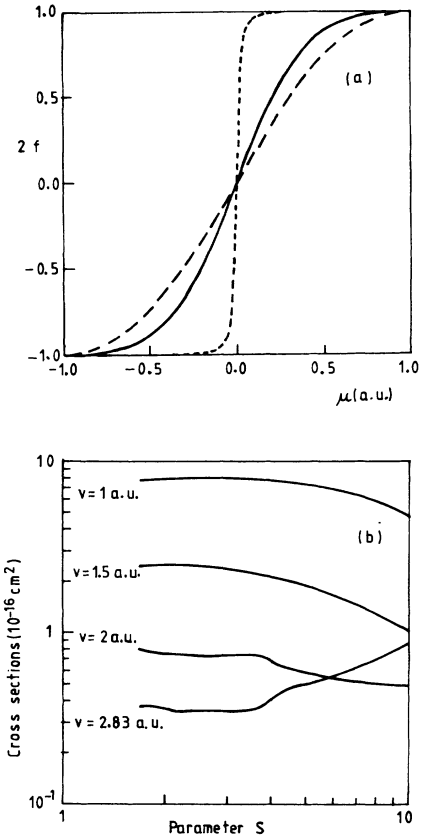

FIG. 1. (a) Switching function $f(\mathbf{r},R)$ of Eq. (19) as a function of the elliptical coordinate $\mu=(r_A-r_B)/R$ for three values of the parameter α: (——) $\alpha=1.25$ ($2S=2.73$); (— — —) $\alpha=11.0$ ($2S=1.69$); (---) $\alpha=1.01$ ($2S=10.3$). (b) Calculated charge-exchange cross sections for reaction (20) using the CTF of Eqs. (16) and (19), and a basis of 23 MO's (Table I), as functions of the gradient of the switching function $f(\mathbf{r},R)$ at the origin, $2S=(\alpha/\alpha-1.0)^{\alpha/2}$, for four values of the impact velocity v (a.u.).

parameter α allows one to modify the switching function from a stepwise form [$\alpha\to 1$, $S\to\infty$, $f\to\frac{1}{2}\,\mathrm{sgn}(\mu)$] to a more slowly varying one [$\alpha\to\infty$, $S\to\frac{1}{2}e^{1/2}$, $f\to\frac{1}{2}\mu$]; see Fig. 1(a).

To determine the value of α we have first employed the norm criterion [18]. However, as could be expected [8], this yields little information at high nuclear velocities, because norms are large and insensitive to the value of α due to the importance of couplings to ionizing channels. The only information obtained is that α should not be too close to unity, because in the $S\to\infty$ limit the norms are found to diverge, some dynamical couplings tending to the square of a δ function. As an additional criterion, we have required that results be stable with respect to small changes in the gradient S. To illustrate this procedure, we display in Fig. 1(b) our calculated charge-exchange cross sections for the reaction

$$^4\mathrm{He}^{2+}+\mathrm{H}(1s)\to{}^4\mathrm{He}^{+}(n=2)+\mathrm{H}^{+} \tag{20}$$

as functions of S for four impact velocities ($v=1$, 1.5, 2, and 2.8 a.u.), using a 23-state MO basis. The results vary little for $0.5<2S<3$, and an intermediate value $2S=2.73$ was selected ($\alpha=1.25$) for the present calculations.

C. PS and $v^{(1)}$ method

As mentioned above, the former method can be introduced as a modification of the PWTF approach in which one ascribes to each MO the same PWTF that corresponds to the entrance channel (i.e., with the electron on center B) instead of Eq. (5). A set of coupled differential equations is then obtained for the expansion coefficients, which can be written in the form of Eq. (17), where the coupling matrix $\mathbf{M}$ is of the form (18) with

$$\mathbf{U}=\mathbf{V}=\mathbf{W}=\mathbf{0} \tag{21}$$

and

$$\begin{aligned} Z_{mn}&=\tfrac{1}{2}\langle\chi_m|-\partial/\partial z|\chi_n\rangle\ , \\ X_{mn}&=(R/2)\langle\chi_m|\partial/\partial x|\chi_n\rangle\ . \end{aligned} \tag{22}$$

The $v^{(1)}$ method can be introduced, starting from the PWTF method, by eliminating the $\exp(\pm i\mathbf{v}\cdot\mathbf{r})$ phases in Eqs. (9), (12), and (13). This yields a system of differential equations that can also be written in the form of Eq. (17) where the coupling matrix $\mathbf{M}$ is of the form (18) with matrices $\mathbf{U}$, $\mathbf{V}$, and $\mathbf{W}$ given by Eq. (21) and

$$Z_{mn}=\begin{cases} \tfrac{1}{2}\langle\chi_m|\partial/\partial z|\chi_n\rangle\ ,\quad X_{mn}=(R/2)\langle\chi_m|-\partial/\partial x|\chi_n\rangle & \text{when } \chi_n\equiv\chi_n^A\ , \\ \tfrac{1}{2}\langle\chi_m|-\partial/\partial z|\chi_n\rangle,\quad X_{mn}=(R/2)\langle\chi_m|\partial/\partial x|\chi_n\rangle & \text{when } \chi_n\equiv\chi_n^B\ . \end{cases} \tag{23}$$

III. MOLECULAR DATA

The molecular basis employed in the PWTF calculations of Ref. [5] was formed by the $1s\sigma$, $2s\sigma$, $2p\sigma$, $3d\sigma$, and $2p\pi$ MO's of the HeH^{2+} quasimolecule. This set is sufficiently small so as to bring forth the effect of the translation factors, and large enough that partial and total charge-exchange cross sections corresponding to the reaction (20) can be calculated. Multiplication of the MO's by PWTF, according to Eqs. (2) and (3), renders the energies and couplings velocity and impact-parameter dependent. Consequently, a complete account of these data would considerably lengthen this article, and we shall only present some representative values. We shall denote the TMO's with the same ($1s\sigma$, $2s\sigma$, $2p\sigma$, $3d\sigma$, $2p\pi$) labels as the original ones. We employed the five-term basis set of these original MO's in our PS and $v^{(1)}$ treatments.

In the CTF calculations we have employed bases formed by 5, 13, 23, and 41 exact MO's, which are listed in Table I. These bases are much larger than the PWTF one for two reasons. First, as mentioned above the CTF method is considerably less time consuming than the PWTF one, and in the latter calculation we cannot increase the MO basis without abandoning the assumption of exact MO's and thereby considerably increasing the

TABLE I. Molecular states of the HeH^{2+} quasimolecule, labeled by their (n,l,λ) united atom quantum numbers, used in the present calculations.

No. of states	HeH^{2+} MO's	Channel
5	210	H(1s) (entrance)
	100	$He^+(1s)$ (capture)
	200, 320, 211	$He^+(n=2)$ (capture)
13	Previous ones plus	
	430, 310, 300, 321, 311	$He^+(n=3)$ (capture)
	420, 540, 431	$H(n=2)$ (excitation)
23	Previous ones plus	
	650, 530, 410, 400	
	541, 421, 411, 432, 422	$He^+(n=4)$ (capture)
	322	$He^+(n=3)$ (capture)
41	Previous ones plus	
	760, 640, 520, 510	
	500, 651, 531, 521	$He^+(n=5)$ (capture)
	511,542,532,522	
	870, 750, 630	$H(n=3)$ (excitation)
	761,641,652	

computational effort. Second, as mentioned in the Introduction, an amount of additional excited states is known to be required in the CTF approach at high energies in order to simulate the effect of "probability absorbers" [8]; we have thus investigated the appropriate choices of these excited states, as well as to the convergence of this "absorbing" procedure. As it is obviously excessive to describe here all the energies and couplings considered, we shall limit our discussion to the CTF data that corresponds to the same minimal basis five MO's treated in our PWTF work.

The energy correlation diagrams corresponding to the five-state basis set are displayed in Fig. 2 for a nuclear velocity $v=2.82$ a.u. and a trajectory with impact parameter $b=0.75$ bohr. We have drawn, as functions of the internuclear distance R, the energies of the unmodified MO's $E_n(R)$ [see Eq. (4)], those of the PWTF TMO's $E_n+(\mathbf{S}^{-1}\mathbf{G})_{nn}$ [see Eq. (14)], and those of the CTF modified MO's E_n+M_{nn} [see Eq. (18)].

With the exception of the $2p\sigma$ state at small distances, differences between MO and TMO energy curves are small, while the M_{nn} terms strongly modify the CTF energies; in particular, the steep increase at short R of the CTF energies will be noticed.

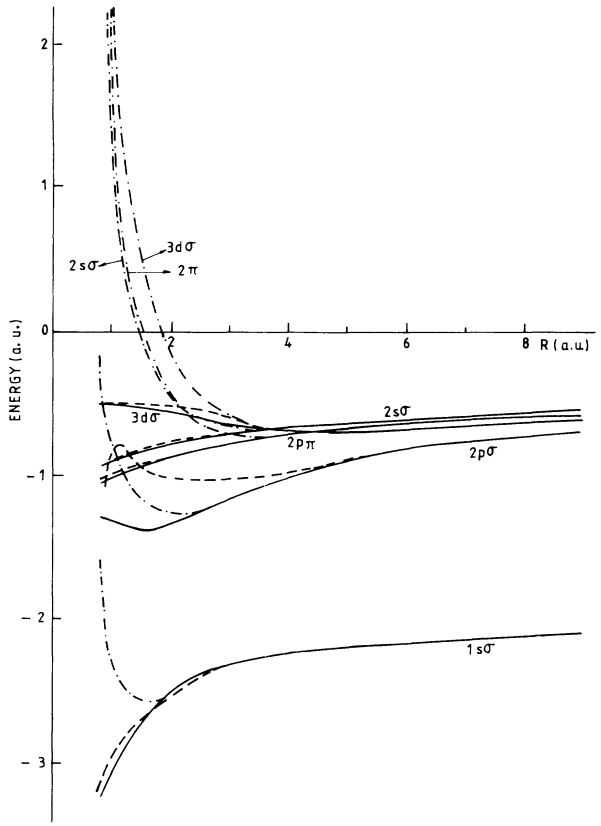

FIG. 2. Energy correlation diagrams corresponding to the five lower MO's of the HeH^{2+} quasimolecule. (——) Electronic energies $E_n(R)$. (— — —) PWTF modified energies: $E_n+(\mathbf{S}^{-1}\cdot\mathbf{G})_{nn}$ [see Eq. (14)], for a trajectory with an impact velocity $v=2.82$ a.u. and impact parameter $b=0.75$ bohr. (—·—·—·) CTF modified energies: E_n+M_{nn} [Eq. (18)] for the same trajectory.

For the same values of v and b as in Fig. 2, we display in Figs. 3(a) $1s\sigma-2p\sigma$, 3(b) $3d\sigma-2p\sigma$, and 3(c) $2p\pi-2p\sigma$ the real and imaginary parts of some representative $\mathbf{S}^{-1}\mathbf{G}$ and $\mathbf{M}$ matrix elements. Since TMO's do not transform like irreducible representations of the $C_{\infty v}$ point group, these dynamical couplings cannot be classified as radial or rotational. For comparison purposes, we include in the figures the values of the corresponding couplings between the original MO's, taking as the origin of electronic coordinates the H nucleus; for the specific couplings considered, this origin coincides with the one chosen in the $v^{(1)}$ approximate method; it also coincides with that for the PS method when the matrix elements of Figs. 3(a)–3(c) are employed in the treatment of reaction (20).

As usual, dynamical couplings are much more sensitive than the energies to modification of the wave functions, and the introduction of translation factors strongly affect those interactions. In addition, for the PWTF approach, the anti-Hermitian character of the couplings is lost.

It may be noticed from Figs. 3(a)–3(c) that the real and imaginary parts of the TMO couplings are of the same order, and strongly oscillate with the internuclear distance. In fact, the same happens for the other matrix elements not shown in these figures. This oscillatory behavior, which will be discussed in Sec. VI, increases with the nuclear velocity and is the main feature that is responsible for the decreasing effectiveness of the couplings with v, and hence for the fall of the charge-transfer cross section. This finding is reminiscent of that of Pfeifer and García [19] in their modification of the Demkov, or exponential, model [19,20] through the introduction of PWTF's.

The modifications in the couplings introduced by the CTF are less spectacular, though also substantial. From Fig. 3 we can also see that, in spite of the v^2 factors that multiply the real part of the interactions [see Eq. (17)], even at the large velocity considered in the figure they are dominated by their imaginary parts, which are proportional to v.

The main conclusion to be drawn from the comparisons in Figs. 2 and 3(a)–3(c) is that the molecular data in the PWTF and CTF approaches are very different from each other, pointing to dissimilar mechanisms.

IV. COLLISIONAL RESULTS

By using a modification of the interpolation and integration algorithms of the program PAMPA [14], as explained and utilized in Refs. [9], [16], and [21], we have integrated the system of coupled differential equations (14) with $\mathbf{S}$ and $\mathbf{G}$ given by Eqs. (8)–(13); and (17) with $\mathbf{M}$ given by Eqs. (18) in the CTF approach, by Eqs. (8), (21), and (22) in the PS method and by Eqs. (8), (21), and (23) in the $v^{(1)}$ method. Our calculated values for the charge-exchange cross section of reaction (20) are given in Fig. 4, and compared to a selection of accurate theoretical results [6,7,9,22–24].

We shall first discuss the PWTF and CTF results. From Fig. 4 we see that at low v our PWTF data are very

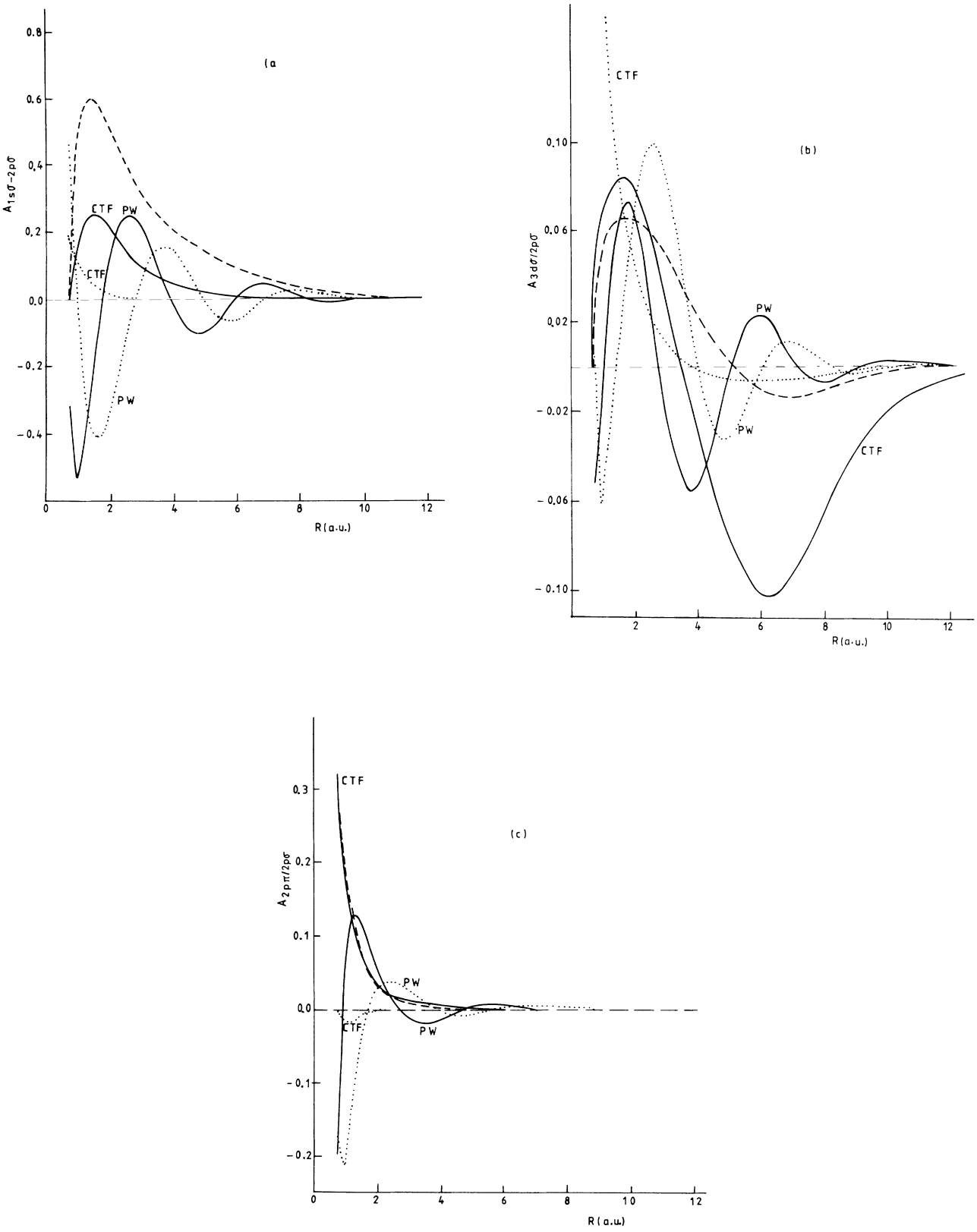

FIG. 3. Imaginary (——) and real (· · · ·) parts of three representative couplings between PWTF (PW) and CTF (CTF) modified MO's as functions of R, for the same trajectory as in Fig. 2. (PW) $(\mathbf{S}^{-1}\cdot\mathbf{G})/v$ matrix elements of Eq. (14); (CTF) M/v matrix elements of Eq. (18). (— — —) Dynamical couplings M/v [M defined by Eqs. (18), (21), and (22)], calculated without translation factors and the origin of electronic coordinates on the proton, used in the PS method. The CTF and PS values in (c) ($2p\pi-2p\sigma$), and the PS values in (b) ($3d\sigma-2p\sigma$) have been multiplied by 0.25 to fit in the figures.

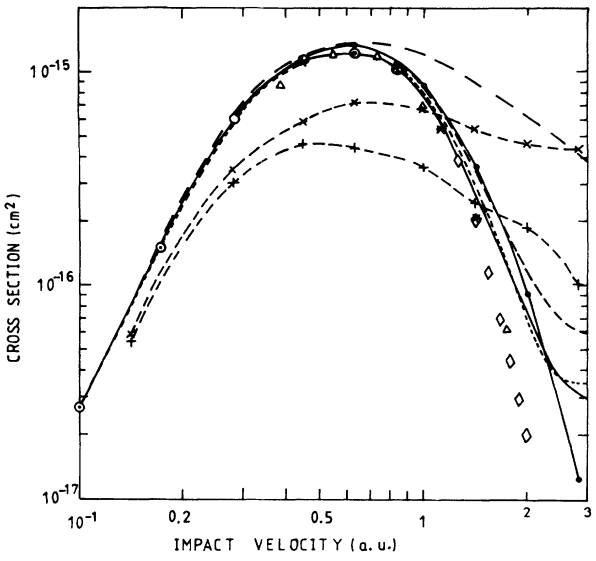

FIG. 4. Charge-exchange cross sections for the $He^{2+}+H(1s)\rightarrow He^{+}(n=2)+H^{+}$ collision as functions of the relative nuclear velocity. (–●–) Present PWTF results obtained integrating the system of differential Eqs. (14) in the basis of 5 MO's (Table I). Present CTF results obtained integrating Eq. (17) in the basis of (see Table I) (— —) 5 MO's; (– – –) 13 MO's; (- - -) 23 MO's; (——) 41 MO's. (–+–) Present PS results obtained integrating the system (17) with M defined by Eqs. (18), (21), and (22) in the basis of 5 MO's. (–×–) Present $V^{(1)}$ results obtained integrating the system (17), M defined by Eqs. (18), (21), and (23) in the basis of 5 MO's. (○) PWTF results of Hatton, Lane, and Winter [6] using 4 MO's ($2p\sigma$, $2s\sigma$, $3d\sigma$, $2p\pi$). (△) PWTF results of Bransden and Noble [22] using an atomic expansion. (◇) Continuum-distorted-wave calculation of Belkic, Gayet, and Salin [24].

close to the corresponding four-state ones of Hatton, Lane, and Winter [6]. This agreement provides a useful check on the accuracy of our calculation, since the numerical procedures adopted by these authors are very different from ours. Further numerical checks were effected with regards to conservation of probability during (and not just after) the collision, and to fulfillment of microreversibility.

From Fig. 4 we may conclude that both PWTF and CTF procedures have converged at low velocities to the correct result, and that, at high velocities, they are able to reproduce the fall of the charge-exchange cross section, provided that a sufficiently large number of MO's is included in the latter method. We also notice that our molecular results are close to those of accurate calculations using atomic expansions [23] with PWTF, and using the continuum-distorted-wave (CDW) approach [24], although they stay higher than these values.

To study the workings of the CTF approach, we performed calculations with bases including up to 41 states. We have drawn in Fig. 4 the results of using 5, 13, 23, and 41 MO bases—each augmentation of the basis set including a new multiplet of states that are degenerate at $R=\infty$. The partial cross sections for the reactions

$$^{4}He^{2+}+H(1s)\rightarrow {}^{4}He^{+}(n=1-3)+H^{+}\ , \tag{24}$$

$$^{4}He^{2+}+H(1s)\rightarrow {}^{4}He^{+2}+H(n=2,3) \tag{25}$$

are also given in Table II for the 41-state CTF calculation, and (whenever possible) by the PWTF one.

We see from these results that, while for $v<1$ a.u. all methods yield practically the same results, for $1<v<2.5$ a.u. cross sections calculated with 5-term PWTF and 23- and 41-term CTF calculations are close, while significant differences are found for the two smallest (5 and 13 MO's) CTF sets. Then, the fact that one obtains a widely different behavior of the cross sections beyond their maximum with a 5-term PWTF, and by a CTF calculation involving the same MO's, requires investigation, especially in view of our previous conclusion (see Sec. III) that the corresponding mechanisms should be rather different.

To illustrate this point, we plot, for the PWTF and 41-term CTF calculations, in Figs. 5(a) $v=0.28$ a.u., 5(b) $v=0.45$ a.u., 5(c) $v=1$ a.u., and 5(d) $v=2.0$ a.u., the values of the opacity function $b|a_i(b)|^2$ vs b, where b is the impact parameter, and $|a_i(b)|^2$ is the exit population through the $He^{+}(n=2)$ states. For $v=0.45$ a.u., we have also included in Fig. 5(b) the ten-state results of Winter and Hatton [7], and the values we obtain in our 5 and 10-state CTF calculations. To complement this information, we show in Fig. 6(a) ($v=0.28$ a.u., $b=3.85$ bohrs), 6(b) ($v=1$ a.u., $b=3.5$ bohrs), 6(c) ($v=2.0$ a.u., $b=1.0$ bohr) the "history" of the collision, that is, the state populations as functions of the Z nuclear coordinate along representative nuclear trajectories.

From Figs. 5(a) and 5(b) we see that 5- and 10-state PWTF, and 5-, 10-, and 41-state CTF, results are close at low velocities, except for trajectories with small impact parameters. It may be noticed that the improvement reached when increasing the MO basis in the CTF and PWTF methods yields results that converge to each other. From Fig. 6(a) we see that the mechanism at low impact energies proceeds through $2p\sigma$-$3d\sigma$ and (to a lesser extent) $2p\sigma$-$2p\pi$ transitions, followed by sharing processes. Transitions to the $1s\sigma$ state are quasinegligible due to the large energy gap involved.

At $v\simeq 1$ a.u. [Figs. 5(c) and 6(b)] this situation is modified in that five-term CTF calculations are no longer accurate. Furthermore, direct $2p\sigma$-$2s\sigma$ transitions become more important than at lower energies and exit populations in the CTF and PWTF begin to differ due to the effect of higher absorber excited states. In both approaches, transitions to the ground state $1s\sigma$ are still negligible because of the energy gap.

At high velocities [Figs. 5(d) and 6(c)], the mechanisms in the CTF and PWTF approach are so different that the methods should be contrasted rather than compared. In the latter approach transitions to the $1s\sigma$ state furnish the primary mechanism and act as a gateway for probability flow to other exit channels. In the CTF approach, the $1s\sigma$ state is much less important, the mechanism being similar as for lower velocities, except that a large amount of states is involved. In fact, the CTF data in Fig. 6(c) is not very informative, since there is a sizable population exit through excited channels that were too numerous to be included in the figure. The importance of

these channels can be gauged by the errors involved in the CTF approach when small bases are used. To unravel the origin of such different, and seemingly complicated, mechanisms, we shall analyze in the following section the workings of both PWTF and CTF molecular models at high impact energies.

We now consider the usefulness of the approximate methods PS and $v(1)$, using five-state calculations. From Fig. 4, the numerical accuracy achieved by those approximations is as follows. For $v<0.3$ a.u. both procedures yield close results, and up to velocities $v=2$ a.u. they both may be considered as being reasonably accurate. The methods fare much worse near the maximum of the cross section than PWTF and CTF calculations. In this region the $v^{(1)}$ method yields better results, although this is probably fortuitous. As expected, neither approximation yields the correct fall of the cross section.

To sum up, our findings with respect to the usefulness of the approximate procedures at energies less than the cross-section maximum is encouraging, especially in view of the extreme simplicity of these calculations. This should, however, be tampered with some information concerning their reliability. Even when reasonable results were obtained, we found ominous warning signs—such as strong lack of microreversibility for the PS method, and large unitarity losses for the $v^{(1)}$ procedure—that the methods should be used with caution. We conclude that further comparative work is needed to check whether the good agreement reached here is fortuitous.

V. HIGH-v BEHAVIOR OF PWTF AND CTF METHODS

We shall now briefly discuss the mechanisms that are responsible for the fall of the charge-exchange cross sections at high impact energies in the CTF and PWTF treatments.

A. PWTF method

In this method the fall is obtained with small bases, so the mechanism must be a simple one. Since the energy phases in Eq. (6) oscillate very little, the dominating coupling is the largest one ($1s\sigma$-$2p\sigma$), independently of the energy gap. The fall of the cross sections follows from the fact that the effectiveness of the $1s\sigma$-$2p\sigma$ matrix element diminishes because of its oscillations as a function of internuclear distance, as explained in the preceding section. The ensuing $1s\sigma$ population is then effectively transferred through direct couplings [Eq. (10)], which do not oscillate. We notice that the mechanism is similar to the corresponding one in an atomic model with PWTF.

A detailed inspection of the molecular data shows that, especially at large R, the $1s\sigma$-$2p\sigma$ TMO matrix element is roughly proportional to $\exp[(i/2)\mathbf{v}\cdot\mathbf{R}]$. To understand the origin of this behavior, we should analyze the structure of the matrix elements of Eqs. (9), (12), and (13). Unfortunately, a closed form of these matrix elements is not available for the exact MO's, and therefore we shall employ in our discussion the expressions obtained from two-center Gaussian expansions [25] of the MO's em-

TABLE II. Calculated partial cross sections ($cm^2\times10^{-16}$) for charge exchange $He^+(n=1-3)+H^+$ and excitation $He^{2+}+H(n=2,3)$ reactions using 41 CTF modified MO's and 5 PWTF modified MO's basis sets as functions of the nuclear velocity v (a.u.). Values in parentheses indicate negative powers of 10.

	$He^+(n=1-3)$ capture					$H(n=2,3)$ excitation	
v	$n=1$ CTF41	$n=1$ PWTF5	$n=2$ CTF41	$n=2$ PWTF5	$n=3$ CTF41	$n=2$ CTF41	$n=3$ CTF41
0.2	1.57(6)		2.44		1.02(1)	0.29(1)	0.01(1)
0.283	3.56(5)	6.86(4)	5.99	6.15	2.80(1)	1.01(1)	0.13(1)
0.3	6.90(5)		6.70		3.53(1)	1.08(1)	0.16(1)
0.346	2.70(4)		8.17		5.02(1)	0.91(1)	0.14(1)
0.4	8.58(4)		10.06		6.13(1)	1.24(1)	0.31(1)
0.447	2.14(3)	2.79(3)	11.22	11.20	7.48(1)	2.08(1)	0.63(1)
0.6	7.86(3)		12.08		1.21	3.15(1)	1.24(1)
0.632		1.36(2)		13.30			
0.7	2.54(2)		11.89		1.46	3.47(1)	1.29(1)
0.8	5.89(2)		10.94		1.80	4.42(1)	1.18(1)
1.0	1.38(1)	1.10(1)	7.68	8.64	2.59	7.87(1)	2.94(1)
1.2	1.83(1)		4.74		2.63	11.36(1)	3.54(1)
1.4	1.85(1)		2.85		2.07	15.23(1)	3.95(1)
1.414	1.84(1)	1.87(1)	2.75	3.63	2.02	15.45(1)	4.00(1)
1.6	1.58(1)		1.74		1.48	17.25(1)	4.60(1)
1.8	1.19(1)		1.09		1.04	17.68(1)	4.97(1)
1.897	1.01(1)		8.95(1)		8.97(1)	17.71(1)	4.91(1)
2.0	8.20(2)	1.69(1)	7.32(1)	9.14(1)	7.79(1)	17.67(1)	4.91(1)
2.2	5.14(2)	1.36(1)	5.23(1)		6.21(1)	17.38(1)	4.84(1)
2.4	2.96(2)		4.08(1)		5.28(1)	16.77(1)	4.85(1)
2.6	1.59(2)		3.51(1)		4.74(1)	15.90(1)	5.05(1)
2.828	8.82(3)	4.35(2)	3.24(1)	1.26(1)	4.12(1)	15.02(1)	4.99(1)

ployed in our calculations:

$$\chi_n = \sum_i C_{ni}\varphi_i \ , \tag{26}$$

where φ_i is a Gaussian-type orbital (GTO) with exponent α_i. Introducing Eq. (26) in Eqs. (9), (12), and (13) then yields expressions for these matrix elements in terms of integrals over traveling GTO's, whose calculation has been described in Refs. [10] and [26]. Taking, as an example, the overlap matrix element we can write

$$S_{nm}^{AB} = \sum_{i,j} C_{ni} C_{mj} F_{ij} \ , \tag{27}$$

and we find that F_{ij} has the form

$$F_{ij} = \exp\left[-\frac{i}{2}\mathbf{v}\cdot\mathbf{R}\right] J_{ij}^{AA} \tag{28}$$

when both GTO's are centered on nucleus A,

$$F_{ij} = \exp\left[\frac{i}{2}\mathbf{v}\cdot\mathbf{R}\right] J_{ij}^{BB} \tag{29}$$

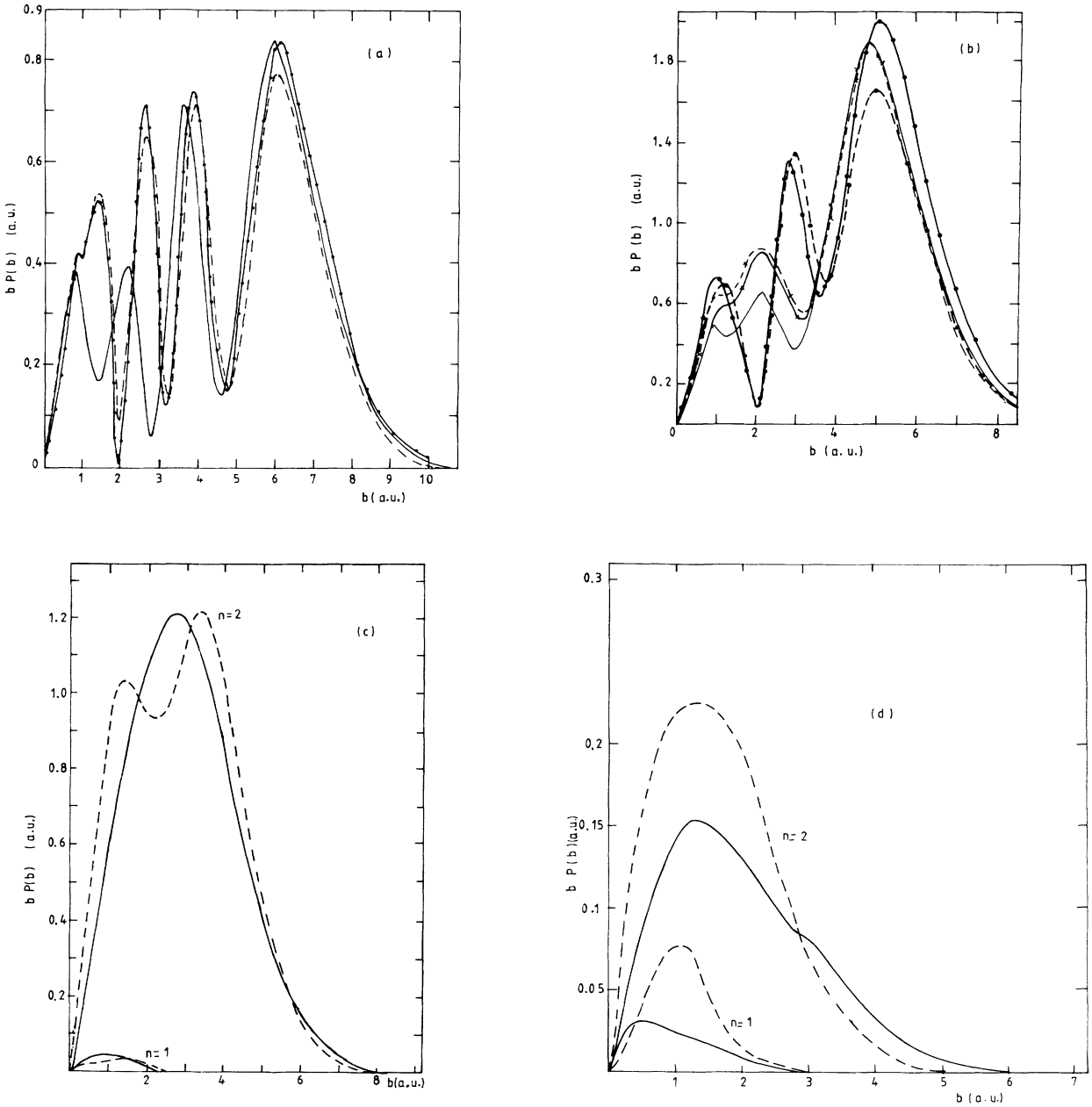

FIG. 5. Charge-exchange probabilities through $He^+(n=1,2)$ exit channels times the impact parameter b, as functions of b for four values of the nuclear velocity. (a) $v=0.28$ a.u.: (— — —) PWTF 5 MO's present results; (—●—) CTF 5 MO's present results; (——) CTF 41 MO's present results. (b) $v=0.447$ a.u.: (-●-) PWTF 5 MO's present results; (—●—) CTF 5 MO's present results; (-×-) PWTF 10 MO's previous results of Winter and Hatton [7]. (—×—) CTF 10 MO's present results; (——) CTF 41 MO's present results. (c) $v=1.0$ a.u. and (d) $v=2.0$ a.u.: (— — —) PWTF 5 MO's present results; (——) CTF 41 MO's present results.

when both are centered on B,

$$F_{ij}=\exp\left[\frac{i}{2}(\alpha_j-\alpha_i)\mathbf{v}\cdot\mathbf{R}/(\alpha_i+\alpha_j)\right]\times\exp[-\alpha_i\alpha_j R^2/(\alpha_i+\alpha_j)]J_{ij}^{AB} \quad (30)$$

when φ_i is centered on A and φ_j on B, and

$$F_{ij}=\exp\left[\frac{i}{2}(\alpha_i-\alpha_j)\mathbf{v}\cdot\mathbf{R}/(\alpha_i+\alpha_j)\right]\times\exp[-\alpha_i\alpha_j R^2/(\alpha_i+\alpha_j)]J_{ij}^{BA} \quad (31)$$

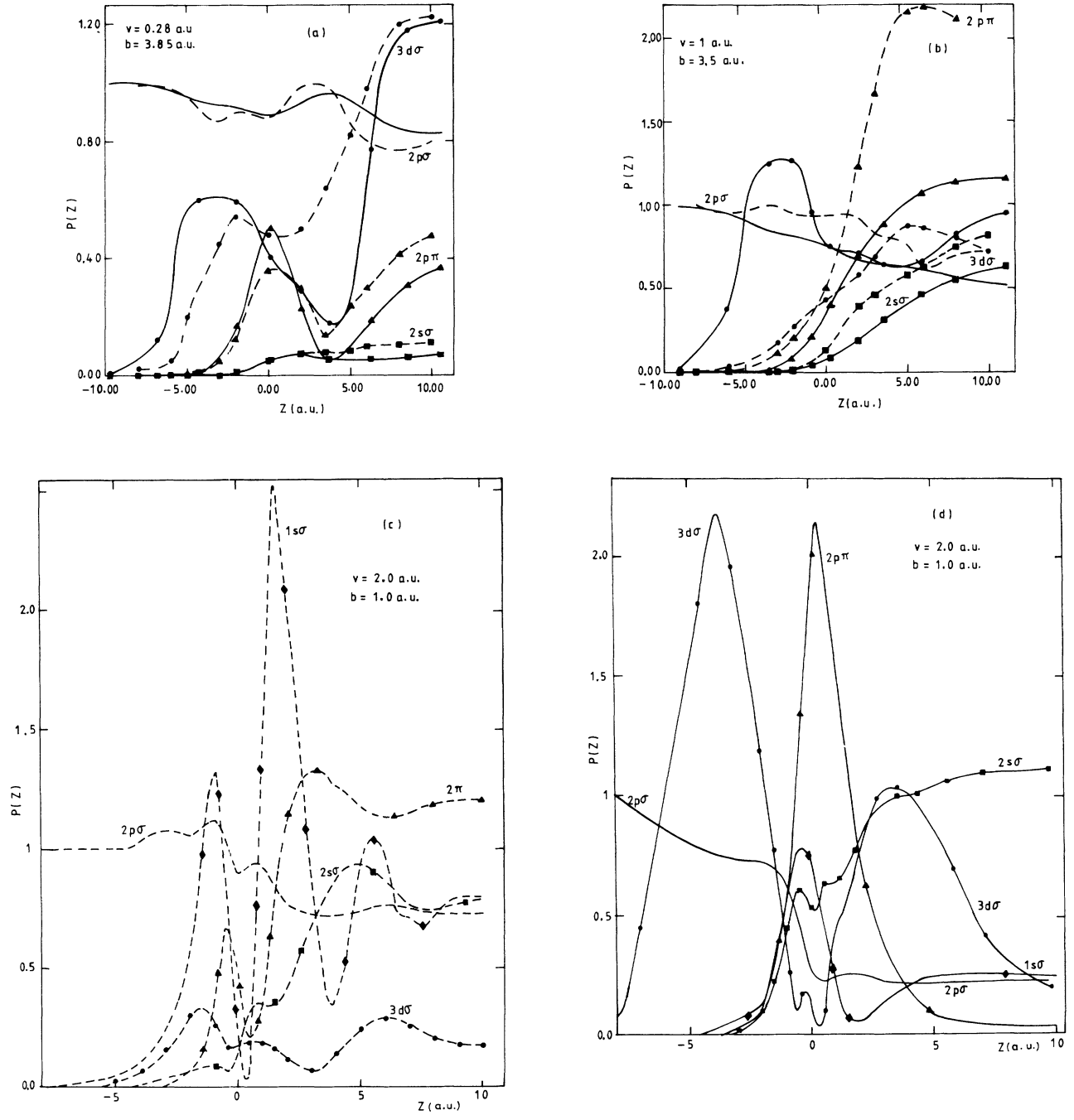

FIG. 6. Population of the entrance channel $2p\sigma$ and charge-exchange $He^+(n=1,2)$ exit channels (multiplied by 10) during the collision as functions of $Z=vt$ along some representative trajectories: (a) $v=0.28$ a.u. and $b=3.85$ bohrs; (b) $v=1.0$ a.u. and $b=3.5$ bohrs; (c) and (d) $v=2.0$ a.u. and $b=1.0$ bohr. (— — —) PWTF 5 MO's present results. (——) CTF 41 MO's present results. Labels are drawn only to help guiding lines. (c) and (d) are presented in two separated drawings (PWTF and CTF results) for the sake of clarity.

in the opposite case. The expressions for J_{ij}, which can be found from Eq. (13) of Ref. [10], show that for $v>1$ a.u. these complex quantities oscillate much less with R than the first factor in Eqs. (28)–(31). When R increases, the behavior of S_{nm}^{AB} depends on which MO, χ_n or χ_m, becomes localized faster. When χ_n is more strongly localized on A than χ_m is on B, the dominant terms will be of type (28) and (30) (with $\alpha_i \gg \alpha_j$), and the phase of F_{ij} will practically be $\exp[-(i/2)\mathbf{v}\cdot\mathbf{R}]$; if χ_m is more strongly localized the dominant terms will be (29) and (30) (with $\alpha_j \gg \alpha_i$) and the phase $\exp[(i/2)\mathbf{v}\cdot\mathbf{R}]$. As a result, local momentum transfer results in that exchange matrix elements display a practically harmonic $\exp[\pm(i/2)\mathbf{v}\cdot\mathbf{R}]$ oscillation. In practice, this "phase locking" begins at quite small ($R \simeq 2$ bohrs) distances, as may be seen in Fig. 7 where the phase of some S matrix elements is given as a function of R for a nuclear trajectory with $v=2.82$ a.u. and impact parameter $b=0.75$ bohr.

The behavior of dynamical couplings (12) and (13) can be explained using similar arguments, by studying the localization of χ_n and $d\chi_m/dt$ instead of χ_n and χ_m. Some representative G matrix elements are also included in Fig. 7, and show that this study is not straightforward: for example, the $3d\sigma$-$2p\sigma$ overlap matrix element is found to oscillate like $\exp[(i/2)\mathbf{v}\cdot\mathbf{R}]$, because the $2p\sigma$ MO localized faster on the H atom than the $3d\sigma$ MO on the He^+ ion, while the opposite situation holds for the $2p\sigma$ MO and the derivative of the $3d\sigma$ MO, with the result that the $3d\sigma$-$2p\sigma$ coupling oscillates like $\exp[-(i/2)\mathbf{v}\cdot\mathbf{R}]$.

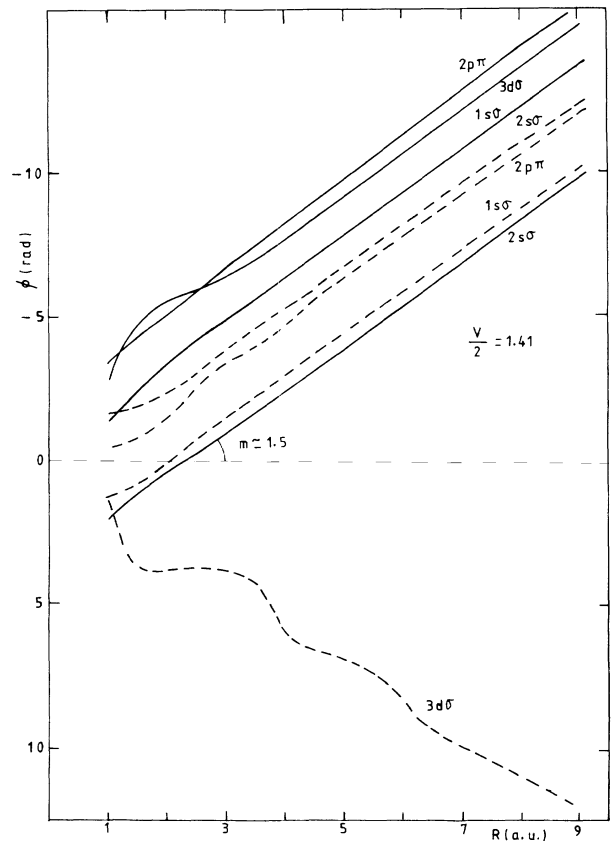

FIG. 7. Phases of S and $\mathbf{S}^{-1}\cdot\mathbf{G}$ matrix elements [see Eq. (6)] between some TMO's, as functions of R, for a nuclear trajectory with $v=2.828$ a.u. and $b=0.75$ bohr. (——) $(\mathbf{S}^{-1}\cdot\mathbf{G})_{J,2p\sigma}$; (— — —) $(S)_{J,2p\sigma}$ ($J=1s\sigma, 2s\sigma, 3d\sigma$, and $2p\pi$).

We have investigated whether our understanding of the origin of the oscillatory behavior of the matrix elements could be employed to improve on the approximate PS or $v^{(1)}$ methods: one could, for example, multiply the dynamical coupling matrix elements by the corresponding phase factor $\exp[\pm(i/2)\mathbf{v}\cdot\mathbf{R}]$. Unfortunately, we were unable to find a simple and general way to determine the relative localization of the derivatives of the MO's, hence to ascertain the phase for the matrix elements (12) and (13). We further checked that use of the wrong phase leads to catastrophic results (for some choices, one even finds oscillating cross sections).

B. CTF method

For this method, rather large bases are required to achieve the correct high-v behavior of the molecular approach. This indicates that the mechanism relies on the complete character of the set of modified MO's $[\exp(iU)\chi_n]$, hence on the convergence of the series (15) when the MO basis is indefinitely enlarged. Nevertheless, how it manages to do so is not obvious at first sight: in order to obtain a complete set, the molecular wave functions corresponding to the ionization continuum should be included; the role of this continuum cannot be negligible at such nuclear velocities that ionization dominates charge exchange; and no continuum wave functions are included in our treatment.

To understand the workings of the method, we first consider the modifications of the molecular data, due to the CTF, at high impact energies. Since the dynamical couplings of Figs. 3(a)–3(c) corresponding to the CTF approach do not show any oscillation, and they are proportional to the nuclear velocity, they increase with v, rather than decrease in the average. This has the effect that many more states become closely coupled at higher, than at lower, velocities. We also see from Fig. 2 that at high velocities the electronic energies are strongly modified by the CTF, especially at small internuclear distances.

A detailed study of the partial cross sections obtained with different basis sets, given in Table II, indicates that the fall in the charge-exchange cross section as v increases is accounted for by a sharing of the probability density among a growing number of states, whose energies E_n+M_{nn} [see Eq. (18)] are more widely separated than those of the unmodified MO's, E_n. In particular, as mentioned in the Introduction, higher excited states act as approximation to "probability absorbers" [8]: Exit population for these states represents genuine probabilities for the corresponding atomic channels, and also probability flux towards even higher—including ionizing—states not included in expansion (15).

Then, in spite of the seeming complexity of our large MO bases, there emerges a simple, and physically meaningful, behavior of the CTF molecular model of atomic collisions at high v. Partial cross sections stabilize (i.e.,

reach a sensibly constant value when the basis set is increased) provided that the basis contains higher excited channels that act as absorbers of probability flux leading to the ionization continuum. When the basis set is further increased, this population is transfered to the next multiplet, and so on. This agrees with an earlier suggestion [27] that a portion of the probability flux which is transferred to the highest-energy MO's corresponds in reality to events in which the electron is gradually detached.

A striking consequence of this ladder mechanism is that, when a molecular calculation is carried out at such high velocities that ionization completely dominates the situation, it should yield, to a good approximation, the ionization cross section, even though no continuum wave functions have been included in the expansion. To illustrate this point we have performed calculations with the 41-state CTF basis up to $v=3.5$ a.u., and in Fig. 8 we have plotted the corresponding cross section for capture into all charge-exchange exit channels (hence, including those acting as "absorbers"). These values may be seen to be very close to the cross section of electron loss by the target (capture plus ionization) measured by Shah and Gilbody [28], and to reproduce the ionization cross section, also shown in Fig. 8, at the higher velocities. These results seem to indicate that the ionization process, in the particular case of $He^{2+}+H$ collisions, is described mainly through a ladder mechanism involving MO's that dissociate into excited states of He^{+}.

A further consequence of this mechanism is that excitation cross sections calculated with the CTF approach should be reasonably accurate at high energies, which is a point that, to our knowledge, has not been studied before. Indeed, this is supported by a comparison, shown in Fig. 9, between our values for the sum of the partial excitation cross sections for reactions yielding $H(n=2,3)$ [Eq. (27)] and other theoretical data [22,23,29]. In particular, for $v<2.2$ a.u. our values are in agreement with those for the total excitation cross section of the atomic calculation of Fritsch, Shingal, and Lin [29], which include states up to $H(n=5)$ as well as pseudostates; at higher velocities our results are a 25% smaller, but present similar variations with the impact velocity.

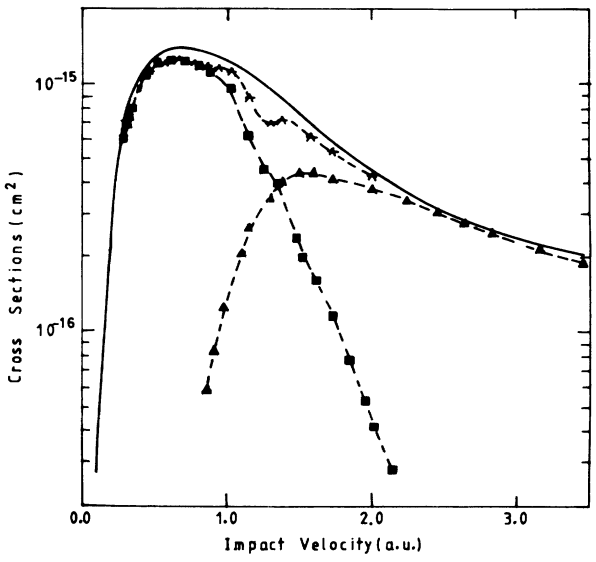

FIG. 8. (——) Charge-exchange cross sections for capture into all $He^{+}(n=1-3)$ channels in $He^{2+}+H$ collisions calculated in the basis of 41 CTF modified MO's. Experimental data of Shah *et al.* [28] for the following. (-■-) Total capture into $He^{+}(\Sigma)$. (-▲-) Ionization cross section. (-*-) Hydrogen electron loss obtained by addition of the previous capture and ionization experimental cross sections.

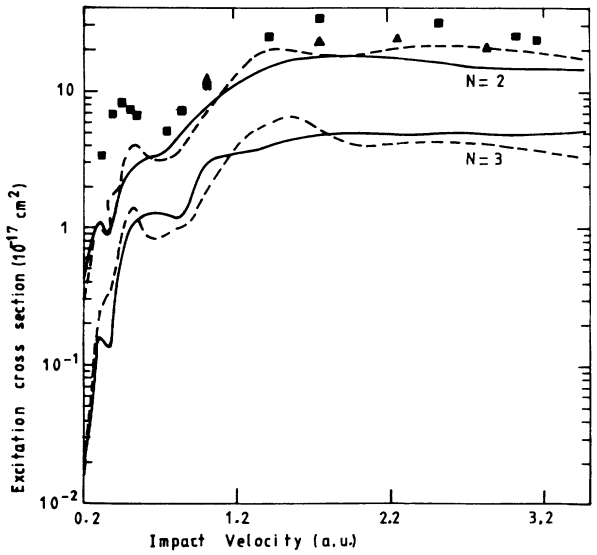

FIG. 9. Calculated cross sections for excitation into $H(n=2,3)$ channels in $He^{2+}+H(1s)$ collisions as functions of the impact velocity. (——) CTF 41 MO's present results; (— — —) Fritsch, Shingal, and Lin [29]; (■) Bransden and Noble [22] results for excitation into $H(n=2)$; (▲) Bransden, Noble, and Chandler [23] results for excitation into $H(n=2)$.

VI. CONCLUSIONS

In the present work, we have complemented a previous letter [5] that showed that the molecular approach, modified with PWTF, is able to reproduce the fall of charge-exchange cross sections in $He^{2+}+H$ collisions, even when using a small basis of MO's. We have presented the relevant molecular data, and explained the mechanism whereby the description of the fall of the cross section is achieved. This mechanism is very similar to that of an atomic expansion with PWTF, in that the momentum transfer coupling matrix elements strongly oscillate with the internuclear distance at high velocities, and therefore cancel on the average.

Because of the computational effort involved in the PWTF approach, we have tested the accuracy of some simplifications that have been employed in the literature. Our conclusions are encouraging for nuclear velocities that are sensibly less than that of the maximum of the charge-exchange cross sections. However, further checks are needed to reach a definite conclusion on the general usefulness of the methods.

We have also investigated whether the success of the PWTF approach is extendable to the widely used CTF method. Our answer is very encouraging, in the sense that using a CTF that is specifically built for high velocities and a MO basis that contains higher excited states that act as "probability absorbers" [8], the fall of charge-exchange partial cross sections is reproduced, as well as the behavior of the excitation cross sections. The success of the CTF method is to be attributed to the convergent character of the molecular expansion modified with the CTF.

An important question arises in the comparison between the PWTF and CTF methods, in that the former would seem, at first sight, to provide a simpler picture of the processes, because it involves fewer MO's. Nevertheless, we have shown that a simple mechanism also emerges from CTF calculations involving as many as 41 MO's; thus, increasing the number of MO's does not prevent a detailed interpretation of the results. Furthermore, this mechanism is capable of describing, at high nuclear velocities, the ionization process. This description occurs through a ladder-type process whereby ionization probability escapes towards the highest excited manifold included in the basis set. This is in agreement with our previous findings [8] employing "probability absorbers" and describes transitions to increasingly diffuse orbitals; it therefore provides a representation of saddle-point electrons [30,31], whereby part of the electronic cloud is left strandled between both nuclei.

We may thus conclude that our findings on the workings of the molecular model of atomic collisions are very encouraging. In particular, the method is not limited to low energies as is usually assumed. Furthermore, we find that the CTF approach is clearly preferable from the computational viewpoint and yields a procedure that provides convergence to partial cross sections (provided absorbing functions are included), a simple picture of the mechanism, and even a description of ionization processes at high velocities.

We should finally mention what seem now to be the two main limitations of the molecular approach, as it has been used here, at high velocities.

One is the difficulty of calculating the (indirect or saddle-point) ionization cross section from the electron-loss data, in the velocity range ($1.2 < v < 2$ a.u. for $He^{2+} + H$ collisions) where change exchange and ionization compete with each other. This is a subject worthy of investigation.

Second, it may be seen from Fig. 4 that the PWTF and 41-state CTF results do not exactly coincide with those of atomic PWTF or CDW calculations. The discrepancy must be attributed to incompleteness of the MO basis in both cases, which may seem surprising in view of the different sizes of the bases in the PWTF and CTF calculations. However, if we consider the mechanisms in both approaches, it is clear that what we cannot describe is the process of direct ionization [31] (as different from saddle-point ionization) due to discrete-continuum dynamical couplings, which lead to direct transitions from the molecular states to the ionizing continuum. The lack of continuum MO's in our bases results in that the probability flux corresponding to direct ionization cannot escape towards the continuum, and an overestimation of the charge-exchange cross section ensues. This picture is in agreement with the findings of Ref. [8], where "probability absorbers" were found to have energies that lie, at small internuclear distances, well into the ionization continuum, and cannot, therefore, be approximated by higher excited bound states. To eliminate this defect, an explicit introduction of these absorbers, or a different way to introduce continuum wave functions in the calculations, seems to be required, but this is beyond the reach of the present work.

ACKNOWLEDGMENTS

This research has been partly supported by the Dirección General de Investigación, Ciencia y Tecnología (Spain), Project No. PB90-0213 and the Centre National Universitaire Sud de Calcul de Montpellier (France).

[1] D. R. Bates and R. McCarroll, Proc. R. Soc. London, Ser. A **245**, 175 (1958).
[2] S. B. Schneiderman and A. Russek, Phys. Rev. **181**, 311 (1969).
[3] C. W. Newby, J. Phys. B **18**, 1781 (1985).
[4] L. F. Errea, L. Méndez, and A. Riera, Z. Phys. D **14**, 229 (1989).
[5] L. F. Errea, J. M. Maidagan, L. Méndez, and A. Riera, J. Phys. B **24**, L387 (1991).
[5] G. J. Hatton, N. F. Lane, and T. G. Winter, J. Phys. B **12**, L571 (1979).
[7] T. G. Winter and G. J. Hatton, Phys. Rev. A **21**, 793 (1980).
[8] L. F. Errea, L. Méndez, and A. Riera, Phys. Rev. A **43**, 3578 (1991).
[9] L. F. Errea, L. Méndez, and A. Riera, J. Phys. B **15**, 101 (1982).
[10] L. F. Errea, L. Méndez, and A. Riera, J. Phys. B **12**, 69 (1979).
[11] R. D. Piacentini and A. Salin, J. Phys. B **7**, 1666 (1974).
[12] J. S. Briggs and K. Taulbjerg, J. Phys. B **8**, 1909 (1975).
[13] A. Riera and A. Salin, J. Phys. B **16**, 2877 (1976).
[14] C. Gaussorgues, R. D. Piacentini, and A. Salin, Comput. Phys. Commun. **10**, 224 (1975).
[15] C. Harel and H. Jouin, J. Phys. B **21**, 859 (1988).
[16] C. Harel and H. Jouin, J. Phys. B **24**, 3219 (1991).
[17] L. F. Errea, J. M. Gómez-Llorente, L. Méndez, and A. Riera, Phys. Rev. A **35**, 4060 (1987); L. F. Errea, J. M. Gómez-Llorente, L. Méndez, A. Riera, C. Harel, and H. Jouin, Europhys. Lett. **6**, 391 (1988).
[18] A. Riera, Phys. Rev. A **30**, 2304 (1984).
[19] S. J. Pfeifer and J. D. García, J. Phys. B **15**, 1275 (1982).
[20] E. E. Nikitin, Adv. Quantum Chem. **5**, 135 (1970).
[21] L. F. Errea, thesis, Universidad Autónoma de Madrid, 1979 (unpublished).
[22] B. H. Bransden and C. J. Noble, J. Phys. B **14**, 1849 (1981).
[23] B. H. Bransden, C. J. Noble, and J. Chandler, J. Phys. B

16, 4191 (1983).
[24] Dz. Belkic, R. Gayet, and A. Salin, At. Data Nucl. Data Tables (to be published).
[25] L. F. Errea, J. M. Gómez-Llorente, L. Méndez, and A. Riera, J. Phys. B **20**, 6089 (1987).
[26] A. Macías and A. Riera, J. Phys. B **11**, 1077 (1978).
[27] M. Kimura and W. R. Thorson, Phys. Rev. A **24**, 1780 (1981).
[28] M. B. Shah and H. B. Gilbody, J. Phys. B **11**, 121 (1978); **14**, 2361 (1981); M. B. Shah, D. S. Elliot, P. McCallion, and H. B. Gilbody, *ibid.* **21**, 2455 (1988).
[29] W. Fritsch, R. Shingal, and C. D. Lin, Phys. Rev. A **44**, 5686 (1991).
[30] R. E. Olson, T. J. Gay, H. G. Berry, E. B. Dale, and V. D. Irby, Phys. Rev. Lett. **59**, 36 (1987).
[31] G. Bandarage and A. Parson, Phys. Rev. A **41**, 5878 (1990).